

# Robust Segmentation and Measurements Techniques of White Cells in Blood Microscope Images

Fabio Scotti

Department of Information Technologies  
University of Milan, Crema, Italy

Phone: (+39) 02 5033-0053, email: fscotti@dti.unimi.it

**Abstract** – The analysis and the count of blood cell in microscope image can provide useful information concerning the health of the patients. In particular, morphological analysis of white cell deformations can effectively detect important diseases such as the Acute Lymphoblastic Leukemia. Blood images obtained by microscopes coupled with a digital camera are simple to obtain and can be more simply transmitted to clinical centers than liquid blood samples. Automatic measurement systems for white cells in blood microscope image can greatly help blood experts that typically inspect blood films manually. Unfortunately, the analysis made by human experts is not rapid and it presents a not standardized accuracy due to the operator's capabilities and tiredness. The presented paper shows how that it is effectively possible to accurately measure the white cells properties in order to allow, at a second stage, the leukemia identification. In particular, the paper presents how to suitably enhance the microscope image by removing the undesired microscope background and a new segmentation strategy to robustly identify white cells permitting to better extract their features for subsequent automatic diagnosis of diseases.

**Keywords** – Blood image analysis, Cell features measurement, White cells identification, Robust segmentation.

## I. INTRODUCTION

The presence of important hematic diseases can be strongly related to modification of the blood components, for example in the modifications in the percentage of blood elements or in their individual morphological features. For example, the Acute Lymphocytic Leukemia (ALL), also known as acute lymphoblastic leukemia is a cancer of the white blood cells and it is characterized by the overproduction and continuous multiplication of malignant and immature white blood cells (referred to as *lymphoblasts* or *blasts*). The observation of the peripheral blood film by expert operators is one of the diagnostic procedures available to evaluate the presence of the acute leukemia [1]. This analysis suffers from slowness and it presents a not standardized accuracy since it depends on the operator's capabilities and tiredness. Conversely, this morphological analysis just requires an image -not a blood sample- and hence is suitable for low-cost, standard-accurate, and remote diagnostic systems.

This paper presents techniques that are required to achieve an automatic classification system to diagnosis the presence of the acute leukemia from blood microscope images. The main

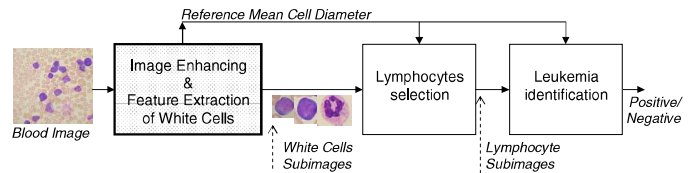


Fig. 1. Modules of an automatic system for acute leukemia detection.

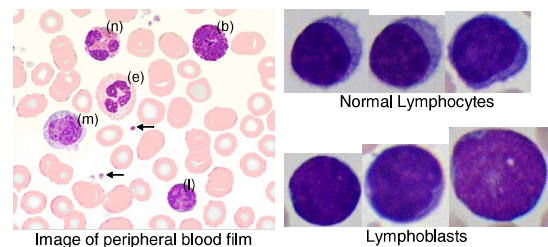


Fig. 2. Left: peripheral blood film with white cells marked with colorant acquired with a microscope. Right: zooms of normal (top) and blast (down) lymphocytes.

modules of the system are sketched in Figure 1. The gray module indicates the module which implements the processing and measurement techniques discussed in this paper. In particular, the paper proposes accurate and robust techniques to measure the property of the white cells in blood microscope image (the one related to the presence of the leukemia) in order to further make automatic classification of the presence of the ALL disease.

The paper is structured as follows. Section 2 focuses on the proposed approach to the problem and compares it with the literature. Then, it shows how it is possible to suitably identify and correct the non-ideal illumination of the microscope image, how it is possible to robustly estimate the mean cell diameter of the cells present in the image (even if they are stacked) and how to properly process segmentation of white cells in the image in order to allow the measurement of cell's properties. Section 3 shows the experimental results obtained by applying the proposed method of a real dataset of images.

## II. THE MEASUREMENT SYSTEM

The proposed sub-system has in input a color image (Figure 1) and it produces in output a list of sub-images containing

one-by-one the white cells present in the input image and an estimation of the mean cell diameter. Subsequent modules of the final system will exploit these outputs to detect the presence of acute leukemia. The system is designed to be capable of processing images grabbed by a commercial digital camera during normal microscope observation of a blood film (Figure 2, left). In the image are present the principal components of blood: basophil (b), eosinophil (e), lymphocyte (l), monocyte (m), neutrophil (n); arrows indicate platelets, other elements are red cells. Figure 2 (right subplots) show the smooth and heterogeneous morphological variations in lymphocytes when acute leukemia is present (area, circularity, compactness, nucleus non-uniformities, etc.). Those features can suitably be measured in the following modules of the final system only if the selection of white cells is accurate and successful.

Only few attempts of partial/full automated systems for leukemia detection based on image-processing systems are present in literature but they are still at prototype stage [2] [3] [4]. Some systems have been proposed as techniques to refine the segmentation (i.e., to solve particular clusters of cells such as in [5] or to refine membrane segmentation as in [6] or to detect incorrect segmentations of white cells as in [7]. In [8] it has been presented a complete classification system to detect acute leukemia from blood images working based only on morphological features and using only gray level images. Even the classification final accuracy was remarkable, the system failed to correctly measure the features of all of the white cells present in the image. Those errors are typically produced by segmentation errors of white cell membranes. The proposed approach aims to make more robust measurement and intelligent segmentation of blood images in order to achieve a high accurate and robust measurement of white cell features. To achieve this goal the system we propose follows three main processing steps:

1. to preprocess the image in order to reduce acquisition noise and background non-uniformities;
2. to estimate the average cell diameter;
3. to perform segmentation with different techniques and combine the results in order to exploit all the available a-priori information achieving a robust identification of white cells.

#### A. Background removal and image enhancing

Our tests show that camera-acquired microscope images of blood suffer from non-uniform background illuminations. Even if the images still remain intelligible, segmentation methods based on thresholding can heavily suffer from this problem. In our approach we identify the background and we subtract it from the original image. The background can be estimated from a *single image* or using a *collection of images* coming from the same microscope and acquisition camera. Both presented techniques are based on gray level images. Many other methods to remove the image backgrounds are present in the literature [9] but most of them have a greater computational complexity, which is not necessary for this application.

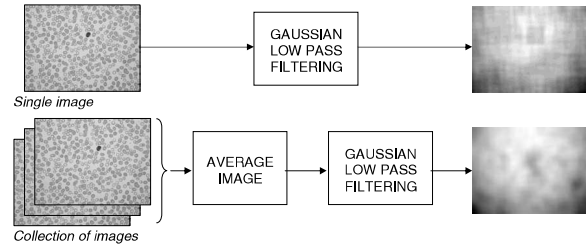


Fig. 3. Background identification by a single image (top) and by using a collection of images (bottom). Background output images are contrast enhanced to better evaluate differences.

In the single image background identification we can assume that the background non-uniformities are larger and smoother than the cells present in the image. That assumption implies that the background has low spatial frequencies than the cells, hence the background can be reconstructed from the image by low-pass filtering the input image. Figure 2 (top) shows the input images (2592x1994) and output of its convolution with a gaussian low-pass filter with the sigma parameter of 400 pixels. In order to reduce the border effects in convolution filtering, no zero-padding has been applied but the image has been duplicated using the mirroring technique.

If it is available a collection of images acquired by the same microscope-camera system (Figure 3), we can compute the mean image. In this case all the contributions of each single cell tend to be averaged, and in the final mean image put in evidence the non-ideal background. Otherwise, if the number of images in the chosen collection is not high (20-40 images), in the mean image is present high-spatial-frequency noise, due to non-perfect suppression of cells. In this case, it is recommended to process a low-pass filtering operation in order to reduce the noise created by the averaging operation. Figure 3 (bottom) shows the results using the approach based on a collection of images.

Once the background image has been reconstructed, it is possible to subtract it from the original image. This operation has two important positive consequences. First of all, it enhances the image removing undesired gray levels belonging to the background and not to the cells. Hence, further contrast enhancement operations will enhance *only* the cells patterns and not the background's tones.

The second positive effect concerns the histogram of the image: after background subtraction the two peaks related to the cell and white background are much more separated, making the histogram to be effectively bi-modal. This will make the segmentation operations based on gray-level thresholding much more robust. In particular, it makes very robust the Otsu-based segmentation method [10] which chooses the threshold of binarization by finding the gray level point where the two peaks distribution in the histogram are better separated. Figure 4 shows the final image and its histogram after background subtraction and contrast enhancing,  $D_1$  and  $D_2$  values show the deepness of the local minima between the two peaks in

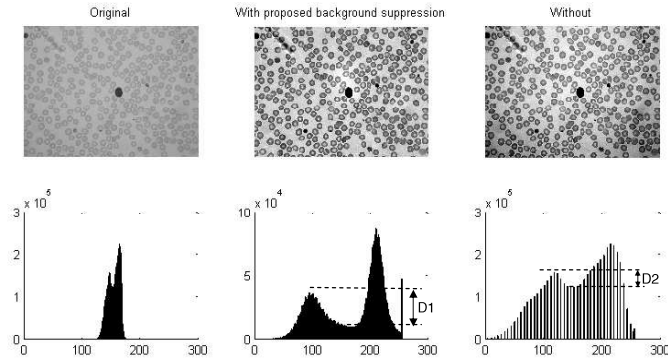


Fig. 4. Effects on histograms of the proposed background suppression. Left: the original image and its histogram. Center: application of background suppression and contrast stretching. Right: only contrast stretching.

the histograms. Since the input image used in Figure 4 has a color depth of 8 bit, it is worth noting that the proposed method (processed in double precision) directly allow to interpolate the intermediate gray levels during contrast stretching operations. Otherwise, directly applying a classical contrast-stretching method on the image, non continuous histograms is produced (Figure 4, right).

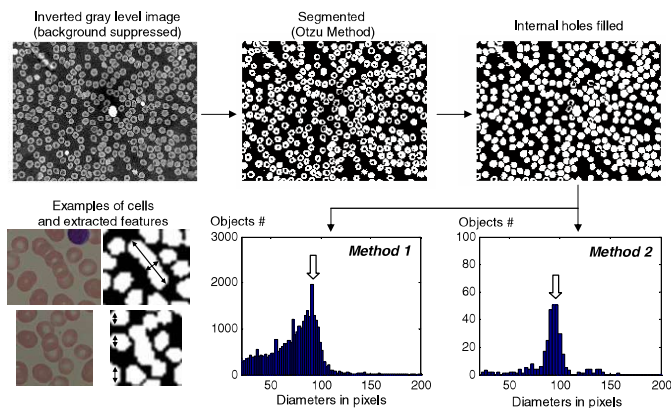


Fig. 5. Top: the processing steps for segmentation. Bottom, left: examples of cells and staked cells; arrows show major and minor axes of an object and segments of objects along a column. Histograms show the distributions obtained by measuring segments on rows and columns (Method 1) and the minor axes (Method 2).

### B. Robust estimation of the cell mean diameter

The acute leukemia typically produces tumoral lymphocytes bigger than normal lymphocytes (Figure 2, right), for this reason is crucial to properly measure the real dimension of white cells. Since it is quite complex to obtain the exact microscope magnification and/or the exact zoom factor of the acquisition camera, it is not possible to obtain the cell measures in microns. It is quite more reliable to measure the dimension of the white cells with respect to the mean cell diameter of cells present in the image as a ratio of dimensions (in pixels). Such procedure allows the system to properly auto-tune without knowing any information concerning the optics during the acquisition. That can be very important when the system is

used in tele-diagnosis or whenever the optical parameters are not directly available.

The measurements of the mean diameter of different circular objects in an image can be processed in by using many techniques [11] [12]. In this application, very often the image contains staked red cells. (cells superimposed and partially overlapping). Hence the shape of objects can also be different from the circular one (Figure 5). We propose two different techniques based on segmentation to be combined in order to process the cell mean diameter. Both technique starts from a binarized image by using automatic thresholding with Otsu method. Our tests shows that the background suppression method presented in section II.A make this operation of segmentation of cells very robust and reliable. Then, the internal holes of segmented objects have to be filled, and object with area minor to a fixed threshold (i.e., 1/600 of the total image area) have to be canceled (Figure 5, top). A first technique can analyzes the distribution of interval lengths of segments equal to 1 (the cells) in the segmented image along rows and columns. Even in the case of staked cells, the most common crossing length in the image corresponds to the mean cell diameter segments. Figure 5 (Method 1) show the distribution of the segments obtained for the plotted image. The position of the largest maximum in the distribution is taken as the value of mean cell diameter. A second technique can be based of the analysis of each object produced by the segmentation and the measurement of its minor axis [13]: in the case of staked cells the major axes can greatly vary depending on the number of cells superimposed and partially overlapping in the stack, but the minor axes it more linked to the real cell diameter (Figure 5, bottom left). The distribution of values of minor axes is then evaluated and the center of the largest maximum is chosen as mean cell diameter (Figure 5, Method 2).

At this stage, the two values returned by the two methods can be combined together, for example by average to compensate the errors.

### C. A robust white cells segmentation method

This subsection focuses on the segmentation methods that can be used to identify the white cells from the input color image. Some important alternatives present in the literature which can be used to segment the cells there are Snakes techniques or Active Contour Models [5], but very often they need some human operator interaction to place initial point or to properly tune some algorithm's parameters according to variation in the input images. Those techniques try to identify pattern in images using contour model built using "a priori" information. In the case of white cells, the difference between types (monocyte, leucocytes, ecc.) are very smooth, hence Active Contour Model methods at present stage of the research are seem to be not very appropriated. They are mostly used to refine the separation of clusters of white cells.

During the preparation of the blood slides, a special marker is used in order to color only white cells with a blue-violet tone. Each slide can assume different marker concentrations

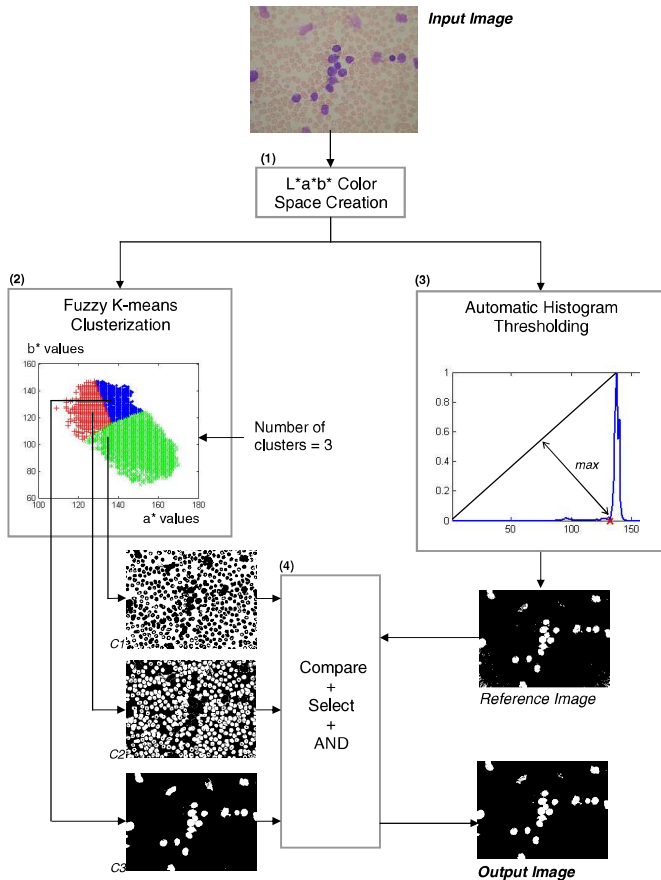


Fig. 6. The proposed segmentation method.

and hence it is not possible to reliably perform segmentation based on a fixed threshold of blue color. Also approaches based only by morphological analysis of cells can often fail the segmentation [8].

This subsection presents the application of a robust method for color segmentation for white cell identification obtained by suitably combine a segmentation based on  $L^*a^*b^*$  color space method [13] with a *gray-level thresholding* method [14]. The combination of the two techniques exploits the advantages of the two methods.

White cells can be identified by human operator by their blue color with respect to the red cells present in the image. This approach is not very robust if it is used to segment white cells since it requires a threshold to decide if a pixel is “more blue than red”. Our tests show that this threshold is not easy to be automatically tuned by the system. In addition, the white cells in a gray-level image are darker than red cells (and than the white background), but again is not easy to automatically process a proper threshold to segment only white cells.

A more robust approach can be based on the analysis of the image  $L^*a^*b^*$  color space (Figure 6, module 1). In  $L^*a^*b^*$  color space,  $L^*$  defines lightness,  $a^*$  denotes red/green value, and  $b^*$  the yellow/blue value. The color space can be un-

pervised clusterized using Fuzzy K-mean clusterization with three centers (Figure 6, module 2) since in the blood image we have three main color: blue (white cells), red (red cells) and gray-white (the background). This clusterization will group the pixels with similar blue/red/white intensities producing three different cluster images ( $C_1$ ,  $C_2$  and  $C_3$  in Figure 6).

The clusterization is fully unsupervised, hence, at this stage, the system must identify which cluster image corresponds to one of white cells. That can be done working with different a priori assumptions, for example, comparing all the three cluster images with a binarization image obtained by gray-level analysis (*reference image*).

In our proposal the reference image is produced by the original image after projection into the  $L^*a^*b^*$  space (using the “ $b^*$ ” channel) and after a thresholding operation using the well-known triangle algorithm of Zack [14]. This method considers the distance of the histogram points with respect to the line passing through the value of the histogram in the origin and its maximum (Figure 6, Module 3). The gray-level level value of the histogram which has the maximum distance from this line is chosen as the threshold for the segmentation.

The cluster corresponding to the white cells is identified by comparing the images of cluster  $C_1$ ,  $C_2$ ,  $C_3$  and the reference image. First of all the proposed algorithm processes a logical AND operation and it selects the cluster image  $C_i$  which has the maximum sum of pixels with one value in the product image. The selected cluster image  $C_i$  has the highest probability to contains the white cells. At this stage the proposed algorithm segments the reference image and it controls if each object in the reference image has a corresponding object in the selected cluster image  $C_i$ . This step is very important since it removes spurious objects present only in the  $C_i$  or only in the reference image (small violet objects, portions of dark red cells, broken white cells, etc.). As final step, all objects in the final output image which has an area minor to half of the mean cell diameter are now removed from the output image.

The result of the proposed algorithm is very “clean” image, where the borders of the white cells tend to be correctly binarized. Notably, the proposed segmentation method has no fixed thresholds, hence it can be considered as fully self adaptive.

That image is the final product of segmentation (the *output image* in Figure 6). At this stage, each segmented white cell can be then analyzed as presented in [8] to determine the presence of the acute leukemia.

### III. EXPERIMENTAL RESULTS

Experiments have been done by using a real dataset of 150 classified images provided by the M. Tettamanti Research Center for Childhood Leukemias and Hematological Diseases Monza, Italy. The dataset permitted to measure the accuracy of the tree main methods presented in this paper: the background suppression, the estimation of the mean cell diameter and the segmentation of the white cells present in the images.

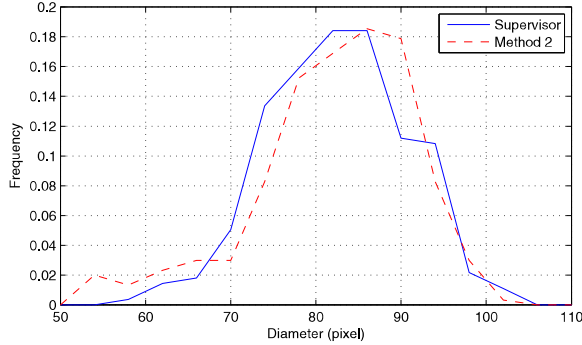


Fig. 7. Distributions of diameters obtained by Method 2 and the supervisor.

### A. Background suppression method

The application of the proposed background suppression method reduced the  $D_1/D_2$  ratio (the ratio of the deepnesses of the local minimum between the two distribution peaks, with or without using the proposed background suppression method) of 182% considering all the images contained in the dataset with respect to considered histogram stretching algorithm. The result shows that the method can effectively enhance the image in order to achieve a more bimodal histogram. Manual observations of the enhanced images confirm a good suppression of non-uniformities of the background.

### B. Mean cell diameter

The accuracy of the algorithm which measures the mean cell radius of cells in the image is not quite simple to be directly measured: unfortunately we do not have the exact distribution of the diameter contained in the images of all the database (more than 15000 cells). Using a so large number of cells it is possible to compare only automatic methods. On the other side, that is not so interesting because it is not possible to identify which method is the more accurate since we do not have a reference measure.

We propose here a different approach to measure the accuracy of the *Method 2* (Figure 5). Our goal is to test if *Method 2* produces a mean cell diameter close to the mean cell diameter given by an expert (Supervisor) which manually measures the diameters of  $N$  cells. In this case we can compare the mean diameter value of *Method 2* with respect to mean diameter value of the supervisor and to apply the Student test in order to verify the congruency of the two mean values.

In Figure 7 we plot the distributions of diameters obtained by *Method 2* and the supervisor obtained with  $N = 243$  cells. The difference between the two means is 0.36 pixel, and the application of the Student Test comparing the two samples (assuming equal variances) produces a significance (using two tails) close to 30% with a 5% confidence interval. This result shows that there is no statistical difference between the two mean diameters values.

The application of this accuracy measurement is not suitable for *Method 1* since the distribution is related to processed segments (Figure 5, left) and not directly to diameters as in the

case of the distribution of *Method 2*. That is demonstrated also by the very different shape of the distribution as can be seen in Figure 5 (bottom right). Interestingly, *Method 1* and *Method 2* present a difference in the diameter estimation of only 0.8 pixels over 250 images (15000 cells).

### C. Segmentation

A qualitative analysis of the output of the segmentation method proposed in Section C is given in Figure 8. The figure plots the output of different techniques processing four different blood images acquired with different experimental situations: definitions (from 2592x1994 to 463x455), bits per pixel (from 24 to 8), different contrast, color saturations and concentration of the violet marker. The methods used in the comparison are the following:

- M1* - Otsu's method on the gray level image;
- M2* - Triangular method on the gray level image;
- M3* - Otsu's method on the  $L^*a^*b^*$  space converted image;
- M4* - Triangular method on the  $L^*a^*b^*$  space converted image (the method to create the *reference image*);
- M5* - final output of the proposed method.

Other segmentation methods based on morphological operators (for example based on watershed and edge detection techniques) have not been considered since they tend to segment all the cells and not only the white cells. Figure 8 shows that the classical approaches based on gray-level thresholding (*M1* and *M2*) are not robust: they segment a lot of red cells instead of only white cells in images with low concentration of the violet marker (such as *I2* and *I3*). That is because, in the gray-level image, some red cells are darker than the white cells colored by the violet marker.

This problem can be effectively solved with the application of the thresholding techniques to the converted image into the  $L^*a^*b^*$  space, (using channel  $b^*$ ) as shown in Figure 8 (*M3* and *M4*). In particular, *M4* represents the method adopted in this paper to create the *reference image*. In our experiments we noted that the Otsu's method (*M5*) tends to segment only the nuclei of the white cells (such as in *I3*). Differently, the application of the Triangular method to the  $L^*a^*b^*$  converted images achieves better results. In both cases we have a lot of spurious objects present in the segmented images (for example traces of dark red cells). This situation can be greatly enhanced using the last processing steps of the proposed method (module 2 and module 4 in Figure 6).

The overall output of the proposed method is given in Figure 8 (*M5*). The segmentation is very effective for all considered images, spurious objects are not present and the borders of the segmented objects suitably follow the edges of the white cells in the original images.

The final white-cell segmentation capability of the proposed method has been evaluated by a human supervisor which evaluated the output of the proposed algorithm checking 200 white cells. The obtained accuracy value is 92%. This analysis enlightens that the proposed method tends to segment also broken

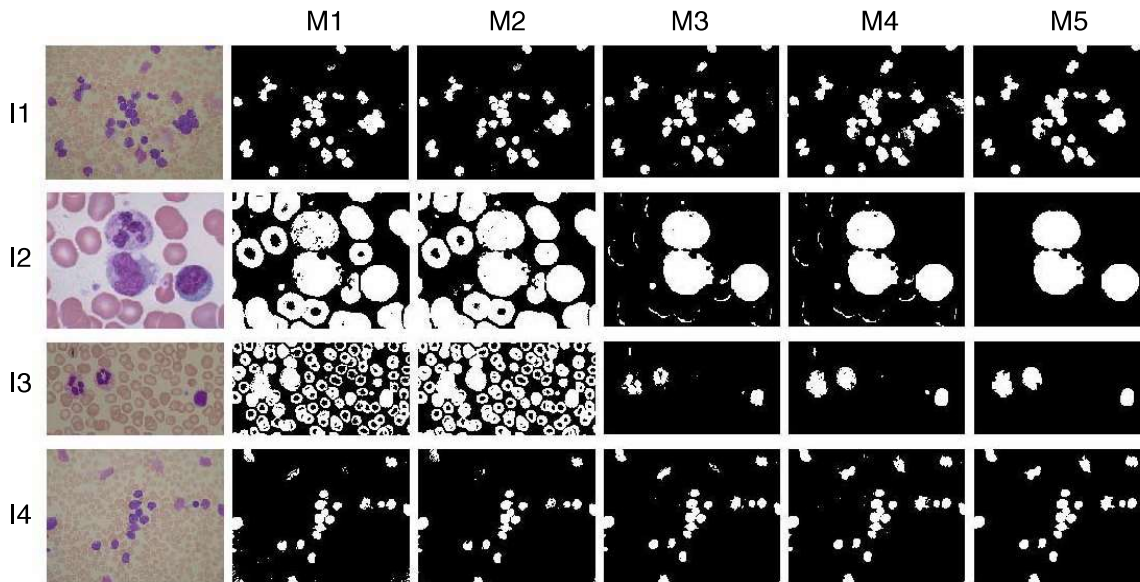


Fig. 8. Comparison of the proposed segmentation method. Four different input images ( $I_1, \dots, I_4$ ) have been binarized with the following methods.  $M_1$ : Otsu's method on the gray level image;  $M_2$ : Triangular method on the gray level image;  $M_3$ : Otsu's method on the  $L^*a^*b^*$  space converted image;  $M_4$ : Triangular method on the  $L^*a^*b^*$  space converted image (the method to create the *reference image*);  $M_5$ : final output of the proposed method.

white cells. This problem can be partially solved in future implementations considering that broken white cells tend to have not the nucleus.

#### IV. CONCLUSIONS

The paper presents different methods to accurately measure cells properties in microscope blood film images. In particular, the paper proposes a method to enhance the microscope images by removing the undesired microscope background, a method for the robust estimation of the mean cell diameter and a new fully self adaptive segmentation strategy to robustly identify white cells permitting. This method allows to easily extract the features of white cells for subsequent automatic diagnosis of blood diseases (i.e., the Acute Leukemia).

#### REFERENCES

- [1] A. Biondi, G. Cimino, R. Pieters, and C. H. Pui, "Biological and therapeutic aspects of infant leukemia," *Blood*, vol. 96, no. 1, July 2000.
- [2] D.S. Serbouti et al., "Image segmentation and classification methods to detect leukemias," in *Proc. International conference of IEEE engineering in Medicine and Biology society*, 1991.
- [3] David J. Foran, Dorin Comaniciu, Peter Meer, and Lauri A. Goodell, "Computer-assisted discrimination among malignant lymphomas and leukemia using immunophenotyping, intelligent image repositories, and telemicroscopy," *IEEE Transactions on Information Technology in Biomedicine*, vol. 4, no. 4, pp. 265–273, 2000.
- [4] K.S. Kim, P.K. Kim, J.J. Song, and Y.C. Park, "Analyzing blood cell image do distinguish its abnormalities," in *Proc. ACM International Conference on Multimedia*, 2002.
- [5] Björn Nilsson and Anders Heyden, "Model-based segmentation of leukocytes clusters," in *Proc. of International Conf. on Pattern Recognition*, 2002, pp. 727–730.
- [6] Q. Liao and Y. Deng, "An accurate segmentation method for white blood cell images," in *Proc. IEEE Int. Symp. on Biomedical Imaging*, 2002.
- [7] P. Bamford and B. Lovell, "Method for accurate unsupervised cell nucleus segmentation," in *Proc. of the Engineering in Medicine and Biology Society Conference*, 2001.
- [8] Vincenzo Piuri and Fabio Scotti, "Morphological classification of blood leucocytes by microscope images," in *Proc. International Symposium on Computational Intelligence for Measurement Systems and Applications*, 2004.
- [9] M. Oberholzer, M. Ostreicher, H. Christen, and M. Bruhlmann, "Methods in quantitative image analysis," *Histochem Cell Biol.*, vol. 105, no. 5, pp. 333–355, May 1996.
- [10] N. Otsu, "A threshold selection method from gray-level histograms," *IEEE Transactions on Systems, Man, and Cybernetics*, vol. 9, no. 1, pp. 62–66, Jan. 1979.
- [11] M. Nixon and A.S. Aguado, *Feature extraction and image processing*, Elsevier, 2005.
- [12] D. H. Ballard, "Generalizing the hough transform to detect arbitrary shapes," *Pattern Recognition*, vol. 13, no. 2, pp. 111–122, 1981.
- [13] R. C. Gonzalez, R. E. Woods, and S.L. Eddins, *Digital Image Processing Using MATLAB*, Pearson Prentice Hall Pearson Education, Inc., New Jersey, USA, 2004.
- [14] G.W. Zack, W.E. Rogers, and S.A. Latt, "Automatic measurement of sister chromatid exchange frequency," *Journal of Histochemistry and Cytochemistry*, vol. 25, pp. 741–753, 1977.